SiO_x Surfaces with Lithographic Features Composed of a TAT Peptide

Youngnam Cho[†] and Albena Ivanisevic*[,†,‡]

Department of Chemistry and Department of Biomedical Engineering, Purdue University, West Lafayette, Indiana 47907

Received: April 14, 2004; In Final Form: July 7, 2004

Synthetic TAT peptides designed to contain an arginine rich basic unit can bind to RNA with an affinity and specificity of a full-length TAT protein. Therefore, deducing strategies to immobilize such short peptides to surfaces can enable one to study their unique recognition properties in various types of sensor platforms. In this paper, we present a strategy to immobilize a 15-residue TAT peptide (CGISYGRKKRRQRRR) in the form of nanoscopic features on SiO_x surfaces. The protocol is based on dip-pen nanolithography that results in the formation of a covalent attachment of the peptide to a SiO_x surface rather than immobilization via electrostatic interactions or patterning on metal surfaces. The nanolithography was characterized by atomic force microscopy (AFM) and X-ray photoelectron spectroscopy. Critical parameters identified by this report include roughness quality and chemical composition of the surface prior to patterning, high humidity conditions, and concentration of ink solution needed to modify the AFM tip. Furthermore, the nanoscopic features were successfully used in recognition experiments where an RNA sequence with a loop structure, known for its specific interaction with the peptide, was tested. The results in this report indicate that one can use nanolithographic strategies to pattern chemically modified "soft" SiO_x surfaces and therefore provide a proof-of-concept experiment that can be transferred in complex microfabricated semiconductor architectures. Developing such patterning methodologies, along with the reported surface characterization protocol, is essential for precise and selective multicomponent placement of biologically active molecules on microcantilever based devices or other types of bio-MEMS platforms.

Introduction

The need to develop platforms to study biochemical events has been recognized by many researchers working in the fields of bioelectronics, biosensing, and biomaterials.[1−4] An example of a versatile platform that has offered alternative routes to high throughput screening and the ability to investigate fundamental (bio)chemical interactions is the development of microarray technologies.[5−7] The advancement in this area has been possible because of the reports of innovative approaches to do efficient surface chemistry immobilization.[8] Through proper surface chemistry routes, researchers have been able to anchor biomolecules (e.g., synthetic DNA, peptides or proteins) to solid supports composed of metal, semiconductor, and polymer materials. The development of such rational methodologies offers many advantages; however, further research is needed with respect to integration with suitable detection methods.[9]

The technology described above often relies on detection methodologies that are based on spectroscopic principles (e.g., fluorescence). One can greatly increase the utility of platforms that allow the investigation of biochemical recognition events if they are based on easier, cheaper, yet more sensitive read-out strategies. Some efforts in this area have centered on incorporating surface immobilization strategies with quartz crystal microbalance experiments[10] and surface plasmon resonance imaging.[11,12] In addition, in the past decade several advances have been made to fabricate devices that can be used to read-out a biochemical event.[13−16] Such microfabricated devices have the potential characteristics that allow them to enable far more efficient, sensitive, and inexpensive chemical identification and data processing strategies. However, the continuous further minituarization of these platforms requires their chemical modification on the nanometer scale with multiple chemical functionalities.[17,18] Such a task calls for unconventional lithographic approaches. Moreover, such site-specific patterning strategies need to be applicable and compatible with established biochemical protocols needed to immobilize biologically important and sensitive molecules.

Several scanning probe microscopy (SPM) based lithography approaches have been reported since the 1990s and have demonstrated the promise to be adapted as a versatile tool to manipulate a variety of molecules, including biomolecules.[19−21] For example, nanografting approaches have been used to immobilize protein and DNA structures on surfaces.[22−25] Another type of scanning probe lithography, dip-pen nanolithography (DPN), has been utilized to pattern various surfaces with a variety of chemical functionalities.[21] The first reports of this technique described patterning of thiols on gold.[26,27] Subsequently, the technique's technological potential was expanded by utilizing silanes or silazanes,[28−30] inorganic sol−gel precursors,[31,32] and polymers and polyelectrolytes[33−37] as inks. In addition, recent reports have shown that biomolecules such as proteins,[38−41] peptides,[42,43] DNA,[44,45] and even viruses[46,47] can be fabricated in ordered surface arrays by DPN. Furthermore, an approach that relied on the biological activity of an enzyme molecule attached to an atomic force microscope (AFM) tip to modify a peptide layer was published.[48] However, very few of the reported scanning probe approaches rely on direct writing and covalent attachment of biomolecules to a solid

* Corresponding author. E-mail: albena@purdue.edu.
[†] Department of Chemistry.
[‡] Department of Biomedical Engineering.

10.1021/jp048359n CCC: $27.50
Published on Web 09/08/2004

substrate.[49] Such an immobilization strategy can offer better control over the point of attachment to a given surface and can lead to a more predictable conformation of the biomolecule on the substrate.

A biochemical event of interest that has been extensively investigated in the literature is the selective binding of RNA to TAT peptides.[50] The protein TAT from human immunodeficiency virus type 1 (HIV-1) has been linked through a variety of studies to important functions in cell permeation and viral replication.[51,52] Researchers have reported experiments that show that short peptide sequences derived from this protein have recognition properties similar to the ones of the whole protein.[53] Therefore, if a proper chemical strategy is designed where the unique recognition properties of the TAT peptides are preserved (i.e., shape), such short sequences can participate in a variety of sensor[50] and in vivo experiments.[54,55]

In this study, we describe how to fabricate nanoscopic features of a TAT peptide on SiO_x surfaces by DPN. Furthermore, we characterize the structures by AFM and X-ray photoelectron spectroscopy (XPS) to verify the presence of peptide on the surface. To test the bioactivity of the fabricated structures, we utilize a sequence-specific RNA and show by XPS that it attaches to a surface containing TAT peptide patterns generated via DPN. The proof-of-concept experiments and characterization protocol we report do not rely on fluorescence measurements and therefore no spectroscopic tags to the biomolecules of interest are needed. Such a characterization protocol can be adapted to microfabricated structures containing both semiconductor and metal surfaces (e.g., surfaces containing gold pads that can easily quench a fluorescence signal).

Experimental Section

Reagents and Materials. Polished silicon wafers with 500 nm of a thermally evaporated oxide film were purchased from Wafer Net, Inc, CA. 3-Aminopropyl-triethoxysilane (APTES), DMSO, concentrated H_2SO_4, and 30% H_2O_2 was purchased from Aldrich. 4-(*p*-Maleimidophenyl)butyric acid *N*-hydroxysuccinimide ester (SMPB), TRIS EDTA buffer at pH ~8.0, and phosphate-buffered saline (PBS) at pH ~6.5 were obtained from Sigma. The TAT peptide sequence (CGISYGRKKRRQRRR) was synthesized by Bio-Synthesis, Lewisville, TX, where it was purified by HPLC and analyzed by MALDI-TOF. The RNA sequence (5′-GGC CAG AUC UGA GCC UGG GAG CUC UCU GGC C-3′) was synthesized, purified, and analyzed by Integrated DNA Technologies, Coralville, IA. Standard solid-phase chemistry protocols were used in both cases.

Surface Preparation. The SiO_x wafer was cut into small pieces of 1×1 cm^2 and cleaned with a piranha solution (3:1 concentrated H_2SO_4: 30% H_2O_2, v:v) for 30 min. Caution: piranha solution reacts violently with organic solvents and should be handled with extreme care! Silanization of the substrates was performed with APTES using a gas-phase method reported by Bein et al.[56] The heterobifunctional cross-linker, SMPB, was coupled to the amine terminated surface by allowing the substrates to incubate in a 1 mM solution of SMPB in EtOH: DMSO (4:1/v:v). Following this step, each surface was rinsed with EtOH multiple times and dried with nitrogen. The cross-linker modified surfaces were incubated for 24 h at 4−8 °C in a 100 μM solution of the TAT peptide prepared in PBS (pH ~6.5). Following this treatment, the surfaces were rinsed several times with the same buffer and washed multiple times with ultrapure water and dried under nitrogen.

Contact Angle Measurements. Static contact angle measurements were performed using a Tantac, Inc Contact Angle Meter (Model CAM-PLUS MICRO) and angles were read by the Half-Angle Method. For each measurement, a drop of water (1 μL) was delivered to the surface using a syringe equipped with a micrometer and the angle was measured within 30 s of the deposition. At least five measurements were done per surface and averaged.

TABLE 1: Summary of the XPS Binding Energy Assignments for C 1s and N 1s after Each Surface Modification Step

surface	C 1s BE (eV); %, assignment	N 1s BE (eV), %, assignment
SiO_x	284.2 (4.5), C−C	
	285.9 (95.5), CH_x	
amine	284.6 (77.2), C−C	399.0 (89.5), NH_2
	286.1 (15.5), C−N	399.8 (10.5), NH_3^+
	287.4 (7.3), C=O	
SMPB	284.4 (52.1), C−C	398.4 (22.3) NH_2
	285.3 (11.4), C−N	399.5 (47.9), amide-N
	286.0 (30.0), amide-C	400.6 (23.3), imide-N
TAT peptide	284.5 (54.8), C−C	398.7 (17.2), NH_2
	285.7 (33), C−N	399.4 (62.8), amide-N
	286.2 (1.4), amide-C	400.2 (19.1), imide-N
	288.0 (10.8), imide-C	401 (0.9), NH_3^+

TABLE 2: Summary of the XPS Binding Energies Assignments for C 1s and N 1s after Patterning with the TAT Peptide and Subsequent Incubation in RNA Solution

surface	C 1s BE (eV); %, assignment	N 1s BE (eV), %, assignment
TAT peptide patterns	284.5 (57.4), C−C	398.6 (13.4), NH_2
	285.6 (20.0), C−N	399.3 (71.5), amide-N
	286.1 (18.6), amide-C	400.4 (8.3), imide-N
	288 (4), imide-C	401.3 (6.8), NH_3^+
TAT peptide patterns + RNA	284.5 (47.2), C−C	
	285.4 (28.3), C−N	399.5 (90.9), amide-N
	286.4 (12.8), amide-C	400.4 (4.9), imide-N
	288.0 (11.7), imide-C	401.9 (4.2), NH_3^+

X-ray Photoelectron Spectroscopy (XPS). XPS survey and high-resolution scans were collected with a Kratos Axis ULTRA X-ray Photoelectron Spectrometer. The instrument was equipped with monochromatic Al Kα X-ray source, small area extraction optics, spherical capacitor electron energy analyzer, and a dual channel plate position sensitive detector. Survey spectra were taken from 0 to 1100 eV with pass energy of 160 eV. High-resolution scans were collected with pass energy of 40 eV. All XPS spectra are plotted on the basis of the intensity obtained from the instrument and are shown as collected to represent signal-to-noise ratios. In figures where the data are presented as stacks, all the plots have the same *y* scales. The data were always collected from the same location on the sample. In experiments where patterned surfaces were used, a micron-sized alignment marker was utilized to ensure that data was collected from the patterned regions. For the XPS evaluation studies, structures were generated next to one another to cover a total area of ~100 μm × 100 μm. The survey and high-resolution scans on the patterned substrates were collected from the same restricted region. Data treatment was done using a commercial software package, XPS PEAK (Version 4.1). The peaks were fitted using a mixture of Gaussian and Lorenzian functions and the background was modeled using a Shirley function. The high-resolution data for C 1s and N 1s were fitted and based on the peak area analysis; percent assignments were made for the components under each element and are summarized in Tables1 and 2.

Atomic Force Microscopy (AFM) and Dip-Pen Nanolithography (DPN). Multi-Mode Nanoscope IIIa from Digital Instruments, equipped with a Nanoscope software system, was

used for all of the DPN patterning experiments and atomic force microscopy (AFM) imaging. The AFM probes used in the experiments, the "V" shaped triangular contact (Model # MSCT-AUHW) and single beam shaped tapping mode tips (Model # OMCL-AC16OTS-W2) were purchased from Veeco Instruments, CA and had spring constants of 0.05 N/m and 42 N/m, respectively. Contact mode AFM was used for the DPN patterning. All the imaging experiments were performed under ambient conditions where temperature and humidity ranged from 20 °C to 24 °C, and 25% to 35%, respectively. Throughout the patterning experiments, the AFM instrument was placed in a home-built glovebox equipped with temperature and humidity controls. To pattern this particular ink, we had to increase the humidity to at least 75% to always obtain consistent and reproducible results. The ink solution in this study was 24 mM TAT peptide dissolved in PBS buffer (pH ~6.5). The tips were coated with peptide by briefly (5−60 s) placing them into an ink solution, rinsing them with buffer, and drying the backside of the cantilever using a clean filter paper. This procedure was repeated multiple times (three to four) prior to the DPN experiments. The tips were immediately mounted onto the AFM tip holder and utilized in the lithography experiments. Prior to the DPN procedure, we calibrated each coated cantilever so that the applied force was 0 nN. This calibration was done at high humidity and by varying the setpoint. We calibrated prior to patterning any given substrate and repeated the calibration if the patterning protocol was longer than 20 min. Two or more patterns with identical dimensions and LFM contrasts, fabricated under the same conditions, were judged as uniform. The patterns consisted of 5−40 lines with lengths of 5 or 10 μm generated using a scan aspect ratio of 256:1. During patterning, the scan parameters were fast scan lines of 512 with scan rates of 3.05 Hz (tip speed of either 30.5 μm/s when 5-μm scan sizes were used or 61.0 μm/s for 10-μm scan sizes). The tip was moved by manually changing the *Y* offset value by increments of 1−2 μm, while the scan direction was kept at 0°. Either lateral force microscopy (LFM) or tapping mode AFM (TMAFM) with clean tips at 90° scan direction was used to verify the DPN patterns, prior to using the substrates for further experiments. LFM and TMAFM images with clean tips were collected under ambient humidity (31−34% humidity). Depending upon the experimental conditions, the imaging was carried out with scan speeds of 2 to 3 Hz.

Results and Discussion

Surface Preparation and Evaluation. Prior to the DPN patterning, we verified that the covalent attachment, Figure 1, of the TAT peptide sequence is feasible using previously documented strategies.[57−61] The immobilization route relies on the success of several coupling reactions. We characterized each surface reaction by contact angle measurement and XPS to assess chemical homogeneity and surface chemical functionality. The surface roughness was assessed using tapping mode AFM. The SiO_x surfaces are expected to experience obvious changes from drastically hydrophilic to hydrophobic during the initial surface modification steps. Therefore, contact angle measurements are a convenient, cheap, and fast way to monitor if a change with respect to the chemical nature of the surface is taking place. The average contact angles were 20°, 60°, 70°, and 30°, for surfaces **1**, **2**, **3**, and **4**, respectively. The trend in these results is in agreement with previously reported studies.[60] The way the contact angle measurements were performed in this study allowed us to gather information regarding the homogeneity of the surfaces on the microscopic level. Furthermore, we monitored the progress of each coupling step by taking contact angle measurements at different times. For example, after the SMPB surface is incubated in the peptide solution for 3−4 h the contact angle changes by only 10−15°, whereas after 24 h it changes by 40°. Incubation in the TAT solution for periods longer than 24 h resulted in surfaces that produced the same change in the contact angle compared to the original SMPB substrates. Such experiments allowed us to determine at what time the maximum possible coverage has taken place. Variable coverages can influence the surface roughness and subsequent success of the patterning protocol (see below). While several different protocols exist in the literature to carry out each step, **1**−**4**, we have found that it is critical to perform the silanization step in the vapor phase.[56] In our studies, we found that compared to surfaces we have silanized in solution, the ones prepared in the vapor phase result in better surface roughness. This result can be caused by a limited multilayer coverage in the case of the vapor phase silanization.

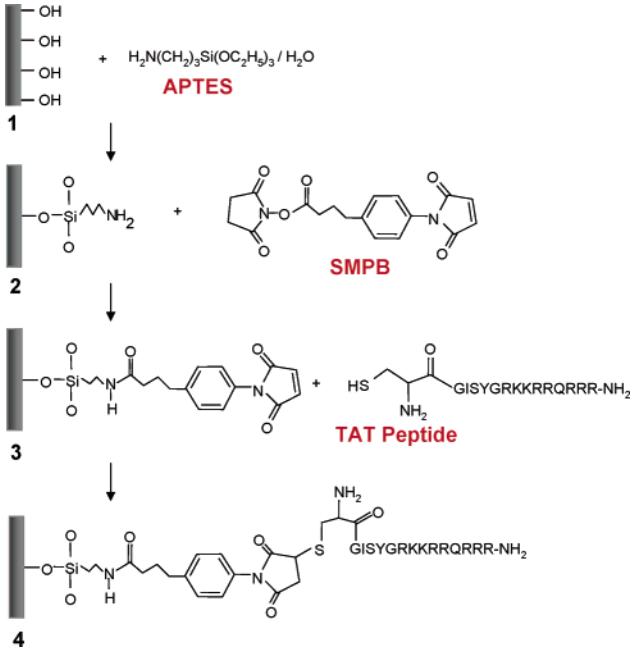

Figure 1. Schematic of surface modification chemistry: (1) Clean SiO_x; (2) preparation of amine terminated surface via silane chemistry with APTES; (3) conjugation of a malemide functionality using a hetero-bifunctional cross-linker, SMPB; and (4) covalent attachment of a TAT peptide via a cysteine residue in the sequence.

The surface roughness after each coupling reaction was determined from tapping mode AFM images taken in air, Figure 2. The RMS values were 0.18, 0.27, 0.38, and 0.37 nm for surfaces **1**, **2**, **3**, and **4**, respectively. These RMS values were calculated by taking five different images on a given surface type, calculating the RMS values, and then averaging them. This AFM analysis is necessary to confirm the consistency in surface morphology upon the completion of each surface reaction. Moreover, it was important to evaluate if the coupling of the TAT peptide resulted in cluster formation. We followed an incubation protocol that is predicted to covalently attach the peptide via a cysteine residue and result in a close to monolayer coverage.[59] A monolayer or less than a monolayer coverage is expected to result in no appreciable changes in the surface morphology. For a variety of applications, this result is beneficial since it allows one to quantify recognition experiments. However, the small change in surface roughness or contrast difference in phase images is not enough to allow one to make valid conclusions regarding the amount of peptide molecules

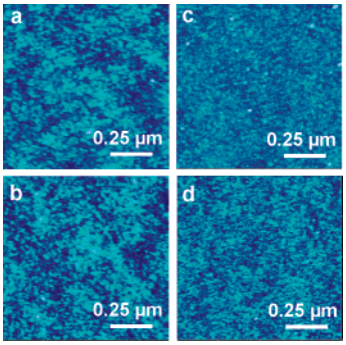

Figure 2. Tapping mode AFM images of (a) Clean SiO_x; (b) APTES modified surface; (c) SMPB modified surface; and (d) TAT peptide terminated surface. These images were collected with a scan size of 1 $\times$ 1 μm^2 and scan rate of 1.97 Hz. The height scale is 10 nm.

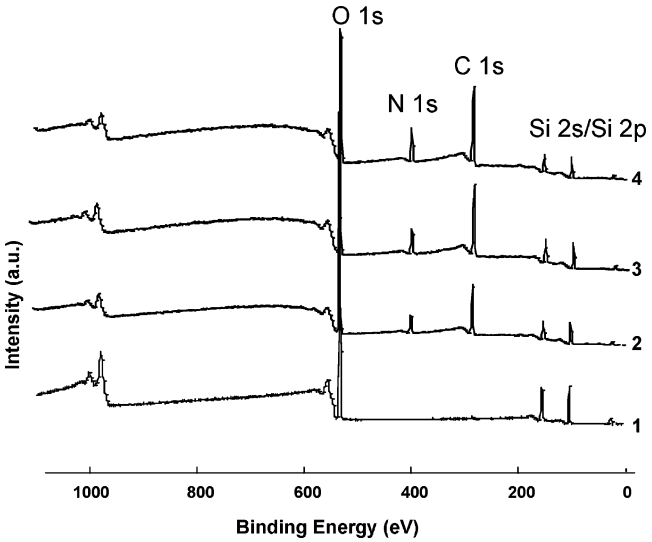

Figure 3. XPS survey spectra of (1) clean SiO_x; (2) APTES modified surface; (3) SMPB modified surface; and (4) TAT peptide terminated surface.

present immediately after incubation or after multiple washings. The main conclusion from these AFM results is that no clustering of the peptide is taking place and, on the basis of the images, we estimate that less than a monolayer of peptide is on the surface. To characterize the chemical nature of the surface in a qualitative or quantitative manner, one needs to use additional surface analysis such as XPS or surface IR.[62]

We selected XPS to evaluate the chemical nature of the surface upon completion of each surface reaction. This type of characterization was chosen over fluorescence based methods because of our desire to use the surface preparation and patterning protocol we report in this study in future experiments involving microfabricated surfaces. The microfabricated surfaces we expect to use will contain multiple types of materials, and in particular the presence of gold structures can quench the intensity of the fluorescence signal significantly.[63] All of the XPS data we collected is in agreement with several related studies previously reported in the literature.[59−61] Survey scans, Figure 3, show the presence of Si 2s, Si 2p, C 1s, N 1s, and O 1s. The relative intensity of C, O, and N gradually increases after each treatment and is in agreement with the surface scheme presented in Figure 1. Since the survey scans can only provide a qualitative understanding of the surface chemistry, we collected high-resolution data for each of the listed elements to quantify the reactions after each treatment. Figure 4a and b shows the stacked data for C 1s and N 1s after each surface reaction. The peaks are centered at the expected binding

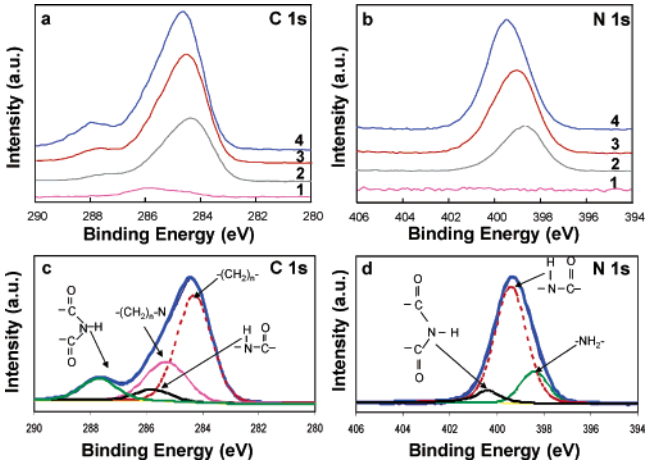

Figure 4. Parts a and b show the high-resolution XPS for the C 1s and N 1s spectra, respectively, after each surface modification step, 1−4. Parts c and d are the results of the XPS surface deconvolution analysis of the TAT terminated surface for C 1s and N 1s, respectively.

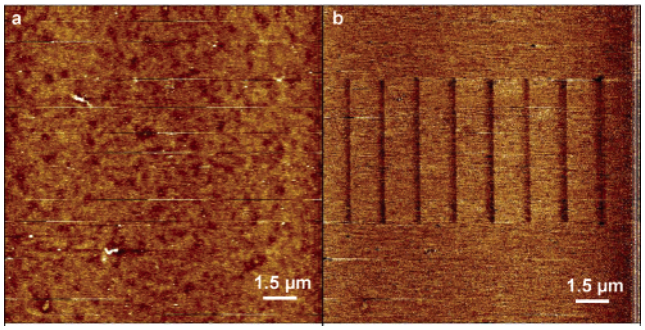

Figure 5. (a) Height and (b) LFM images of an SMPB terminated surface containing DPN patterns terminated with a TAT peptide. Both images were collected with a scan size of 11.06 $\times$ 11.06 μm^2 and scan rate of 3.05 Hz. The LFM data scale is 40 mV and the height scale is 5 nm. The widths of the first and last line from left to right are 200 and 375 nm, respectively.

energies, 285.0 and 400.0 eV, for C 1s and N 1s, respectively. However, both peaks are broad and therefore can be deconvoluted, Figure 4c and d. The deconvolution was done using commercially available software and revealed the presence of several different species after each treatment. A summary of the deconvolution results is presented in Table 1. The trends in these data are the following: (i) the C 1s data displays an additional component after SMPB and TAT attachment in the 288.0 eV region because of the coupling of amide/imide functionalities and (ii) the N 1s data always reveals a broad peak that is initially centered at 399.0 eV (predominately because of protonated and nonprotonated amines) and then shifts to 400.0 eV in agreement with the presence of amide/imides on the surface.[57,58] The surface preparation procedure we described in the Experimental Section and evaluated through the techniques discussed in this section allowed us to obtain the results summarized in Table 1 reproducibly and was critical to the success of the patterning protocol detailed below.

DPN of a TAT Peptide. Upon the validation of the coupling chemistry we described in the previous section, we utilized the SMPB terminated surface to fabricate nanoscopic features composed of a TAT peptide by DPN, Figure 5. We expect that the TAT peptide is not lying flat on the surface. Such orientation is important in biorecognition experiments. Throughout this study, several key issues were identified and the absence of any one of them resulted in irreproducible surface patterning. These issues are (i) initial surface quality; (ii) the calibration of

the cantilever in order to apply minimum force with the tip; (iii) critical amount of "ink" molecules on the tip; and (iv) high humidity conditions. Details regarding the first issue were presented in the previous section. In this part of the paper, we elaborate on the other three parameters that are necessary to pattern the TAT peptide via DPN with the resolution shown in Figure 5.

The SMPB terminated surface we utilized to do the patterning is fairly hydrophobic (contact angle of 70°). In addition, this surface is "soft"; because of the number of surface reactions performed it is easy to indent it if higher loads are applied during scanning. Previous attempts to pattern peptides on modified surfaces in contact mode were unsuccessful because of high surface roughness and nonuniformity of the coating.[43] After we optimized our protocol to obtain homogeneous and relatively smooth surfaces (RMS $<$ 1 nm), we were able to calibrate our coated cantilever so that the minimum amount of force was applied during the DPN procedure. This calibration is necessary for each different cantilever used. As the amount of ink depletes from the tip, it is necessary to readjust the setpoint to obtain uniform patterns over longer periods of time. When the lowest possible setpoint is used that allowed the tip to come into contact with the surface, no scratching of the modified SiO_x was observed, Figure 5a. Imaging the patterns in contact mode allows to confirm the patterning via the LFM image, Figure 5b, but can cause damage and compression to the TAT peptides and thus prevent their visualization as 1−2-nm tall features in the height image. In our earlier studies when we did not optimize the coupling chemistry shown in Figure 1, we were unable to pattern the TAT peptides in contact mode. Furthermore, a critical amount of ink on the tip is necessary to obtain uniform patterns. Several different reports in the literature exist that detail how to make the tip hydrophilic and induce greater adsorption of ink molecules.[38,39,49] In this study, we coated the silicon nitride tip multiple times in a solution of TAT peptide with very high concentration. This allowed us to first irreversibly physisorb enough peptide on the tip to make it more hydrophilic and then adsorb an additional amount of peptide on it that can be transferred on the surface during the DPN process. The most likely mechanism of the irreversible physisorption of the ink to the tip is via weak interactions among the ink molecules (e.g., dipole interactions or dispersion forces). In addition, we discovered that regardless of the amount of ink present on the cantilever, because of the high hydrophobicity of the modified SiO_x very few molecules transfer at humidity between 10 and 50%. Our best patterning results were obtained when the humidity was kept between 78 and 80%. Similar results are observed with protein molecules.[38,39,49] The most likely mechanism of this hydrophilic ink transport to a hydrophobic surface is one dominated by molecular deposition rather than lateral diffusion or surface binding events as described by Jang et al.[64] To verify this hypothesis, a more comprehensive study is needed and we plan to report the results from it in the future. Furthermore, in future studies, we plan to investigate in detail the transport properties of these molecules on hydrophobic and hydrophilic surfaces. The transfer of TAT peptide molecules under our experimental conditions is slow and one needs to scan over the same line multiple times to deliver enough material to see differences in the LFM images or phase contrast in tapping mode images. A possible way to improve the efficiency and throughput of this process is to use microfluidic tips.[65]

To confirm that the patterns we generated are stable and not just due to the transfer of salt present in the buffer, we "aged" the patterned surfaces at 4 °C for 24 h to allow the coupling chemistry to take place, washed them with water several times, and imaged them with a clean tip. This stability experiment however is not enough to conclude that the DPN process was successful. If the patterned surfaces were not allowed to age for the coupling chemistry to take place, we were able to wash away the fabricated structures. In any type of lithography with biological molecules, one needs to evaluate the size, chemical composition, and conformation of the generated features. The size can be extracted from the AFM data. The smallest feature we have been able to write had a width of 100 nm. We assessed the chemical composition by using XPS and performed a biological activity test that allowed us to determine if the peptide is immobilized onto the surface in a conformation that allowed it to participate in a sequence specific interaction with a loop RNA sequence.

Several instrumentation advances have improved the spatial resolution of XPS.[66] For the instrument we used (see Experimental Section), a larger area needed to be patterned to successfully evaluate the elemental composition of the DPN TAT patterns. We used a micron size alignment marker on the surface to pattern an area of ∼100 μm × 100 μm and then collected survey and high-resolution spectra from this restricted region. The high-resolution data was deconvoluted as described in the previous section and the results are summarized in Table 2. The presence of the amide-N species in the N 1s spectra and the C−N species in the C 1s spectra are consistent with the adsorption of the peptide on the surface. The patterned surfaces were then incubated in 5 μM solution (TRIS buffer at pH ∼8.0) of TAR RNA and analyzed by XPS. TAR RNA binding to short peptide sequences derived from the TAT protein has been studied by others.[50] Such studies have shown binding specificity and have been in agreement with experiments done with the TAT protein.[67] We used the exact same hairpin RNA of 31 bases that Tassew et al.[50] have utilized in an acoustic wave sensor study. Our XPS data, Table 2, collected after the patterned surface was incubated in the TAR RNA solution, indicates that more amide species are present on the surface. The comparison between the data for the two types of substrates summarized in Table 2 allows us to conclude that our patterns can recognize the TAR RNA sequence. In control experiments, we have immobilized the TAT peptides on 1 × 1 cm surfaces prepared by the protocol outlined in Figure 1 and have then incubated them in TAR RNA solution. The data we collected from these two types of surfaces matches the data in Table 2. Furthermore, in areas where no TAT peptide patterns were placed we did not record any of the observations summarized in Table 2. However, strictly speaking, the XPS experiments do not allow us to completely exclude the possibility that the presence of RNA or TAT peptide molecules on the surface is simply due to electrostatic interactions. Therefore, recognition experiments involving multiple types of RNA and peptide sequences are underway in our laboratory. Such experiments can help us understand the conformation of different peptides on a surface after the DPN procedure and correlate it with their biological activity and recognition properties.

Conclusions

In summary, we demonstrate a procedure to prepare hydrophobic substrates suitable for DPN writing. Such surfaces have been successfully utilized in patterning experiments where peptide molecules were attached covalently to the surface. This study utilizes a characterization protocol that does not depend on fluorescence measurements and can therefore be adapted in

evaluating the patterning of complex architectures such as microfabricated structures. Furthermore, the patterns generated via DPN can be used in biorecognition experiments and open the possibility of incorporating multiple types of peptides in new detection platforms (e.g., MEMS devices) where unconventional patterning approaches are advantageous.

Acknowledgment. This work was supported by the Bindley Biosciences Center (BBC) at Purdue University and by NASA under award No. NCC 2-1363. Any opinions, findings, and conclusions or recommendations expressed in this material are those of the authors and do not necessarily reflect the views of the National Aeronautics and Space Administration. The authors acknowledge experimental help from Dr. Richard Haasch (UIUC) to carry out the XPS characterization. All XPS experiments were performed at the Center for Microanalysis of Materials, UIUC, which is partially supported by U.S. Department of Energy under grant DEFG02-91-ER45439.

Supporting Information Available: Friction image of a SMPB terminated surface containing DPN patterns composed of a TAT peptide. This material is available free of charge via the Internet at http://pubs.acs.org.

References and Notes

(1) Hirano, Y.; Mooney, D. J. *Adv. Mater.* **2004**, *16*, 17−25.
(2) Zhang, S. *Nature Biotech.* **2003**, *21*, 1171−1178.
(3) Niemeyer, C. M. *Angew. Chem., Int. Ed.* **2001**, *40*, 4128−4158.
(4) Mrksich, M.; Whitesides, G. M. *Trends Biotechnol.* **1995**, *13*, 228−235.
(5) Templin, M. F.; Stoll, D.; Schrenk, M.; Traub, P. C.; Vohringer, C. F.; Joos, T. O. *Trends Biotechnol.* **2002**, *20*, 160−166.
(6) Houseman, B. T.; Mrksich, M. *Trends Biotechnol.* **2002**, *20*, 279−281.
(7) Lee, Y. S.; Mrksich, M. *Trends Biotechnol.* **2002**, *20*, S14−S18.
(8) MacBeath, G.; Schreiber, S. L. *Science* **2000**, *289*, 1760−1763.
(9) Kolusheva, S.; Kafri, R.; Katz, M.; Jelinek, R. *J. Am. Chem. Soc.* **2001**, *123*, 417−422.
(10) Furusawa, H.; Murakawa, A.; Fukusho, S.; Okahata, Y. *ChemBioChem* **2003**, *2*−*3*, 217−220.
(11) Wegner, G. J.; Lee, H. J.; Corn, R. M. *Anal. Chem.* **2002**, *74*, 5161−5168.
(12) Shumaker-Parry, J. S.; Aebersold, R.; Campbell, C. T. *Anal. Chem.* **2004**, *76*, 2071−2082.
(13) Fritz, J.; Baller, M. K.; Lang, H. P.; Rothuizen, H.; Vettiger, P.; Meyer, E.; Guntherodt, H. J.; Gerber, C.; Gimzewski, J. K. *Science* **2000**, *288*, 316−318.
(14) Hansen, K. M.; Ji, H. F.; Wu, G.; Datar, R.; Cote, R.; Majumdar, A.; Thundat, T. *Anal. Chem.* **2001**, *73*, 1567−1571.
(15) Yang, Y.; Ji, H. F.; Thundat, T. *J. Am. Chem. Soc.* **2003**, *125*, 1124−1125.
(16) Pei, J.; Tian, F.; Thundat, T. *Anal. Chem.* **2004**, *76*, 292−297.
(17) Pinnaduwage, L. A.; Hawk, J. E.; Boiadjiev, V.; Yi, D.; Thundat, T. *Langmuir* **2003**, *19*, 7841−7844.
(18) Lang, H. P.; Berger, R.; Andreoli, C.; Brugger, J.; Despont, M.; Vettiger, P.; Gerber, C.; Gimzewski, J. K.; Ramseyer, J. P.; Meyer, E.; Guntherodt, H. J. *Appl. Phys. Lett.* **1998**, *72*, 383−385.
(19) Kramer, S.; Fuierer, R. R.; Gorman, C. B. *Chem. Rev.* **2003**, *103*, 4367−4418.
(20) Liu, G. Y.; Xu, S.; Qian, Y. *Acc. Chem. Res.* **2000**, *33*, 457−466.
(21) Ginger, D. S.; Zhang, H.; Mirkin, C. A. *Angew. Chem., Int. Ed.* **2004**, *43*, 30−45.
(22) Wadu-Mesthrige, K.; Amro, N. A.; Garno, J. C.; Xu, S.; Liu, G. Y. *Biophys. J.* **2001**, *80*, 1891−1899.
(23) Wadu-Mesthrige, K.; Xu, S.; Amro, N. A.; Liu, G. Y. *Langmuir* **1999**, *15*, 8580−8583.
(24) Liu, M.; Amro, N. A.; Chow, C. S.; Liu, G. Y. *Nano Lett.* **2002**, *2*, 863−867.
(25) Zhou, D.; Wang, Z.; Birch, L.; Rayment, T.; Abell, C. *Langmuir* **2003**, *19*, 10557−10562.
(26) Piner, R. D.; Zhu, J.; Xu, F.; Hong, S.; Mirkin, C. A. *Science* **1999**, *283*, 661−663.
(27) Hong, S.; Zhu, J.; Mirkin, C. A. *Langmuir* **1999**, *15*, 7897−7900.
(28) Jung, H.; Kulkarni, R.; Collier, C. P. *J. Am. Chem. Soc.* **2003**, *125*, 12096−12097.
(29) Pena, D. J.; Raphael, M. P.; Byers, J. M. *Langmuir* **2003**, *19*, 9028−9032.
(30) Ivanisevic, A.; Mirkin, C. A. *J. Am. Chem. Soc.* **2001**, *123*, 7887−7889.
(31) Su, M.; Liu, X.; Li, S. Y.; Dravid, V. P.; Mirkin, C. A. *J. Am. Chem. Soc.* **2002**, *124*, 1560−1561.
(32) Fu, L.; Liu, X.; Zhang, Y.; Dravid, V. P.; Mirkin, C. A. *Nano Lett.* **2003**, *3*, 757−760.
(33) Noy, A.; Miller, A. E.; Klare, J. E.; Weeks, B. L.; Woods, B. W.; DeYoreo, J. J. *Nano Lett.* **2002**, *2*, 109−112.
(34) Lim, J. H.; Mirkin, C. A. *Adv. Mater.* **2002**, *14*, 1474−1477.
(35) McKendry, R.; Huck, W. T. S.; Weeks, B.; Fiorini, M.; Abell, C.; Rayment, T. *Nano Lett.* **2002**, *2*, 713−716.
(36) Maynor, B. W.; Filocamo, S. F.; Grinstaff, M. W.; Liu, J. *J. Am. Chem. Soc.* **2002**, *124*, 522−523.
(37) Nyamjav, D.; Ivanisevic, A. *Adv. Mater.* **2003**, *15*, 1805−1809.
(38) Lee, K. B.; Lim, J. H.; Mirkin, C. A. *J. Am. Chem. Soc.* **2003**, *125*, 5588−5589.
(39) Lim, J. H.; Ginger, D. S.; Lee, K. B.; Heo, J.; Nam, J. M.; Mirkin, C. A. *Angew. Chem., Int. Ed.* **2003**, *42*, 2309−2312.
(40) Agarwal, G.; Naik, R. R.; Stone, M. O. *J. Am. Chem. Soc.* **2003**, *125*, 7408−7412.
(41) Hyun, J.; Ahn, S. J.; Lee, W. K.; Chilkoti, A.; Zauscher, S. *Nano Lett.* **2002**, *2*, 1203−1207.
(42) Wilson, D. L.; Martin, R.; Hong, S.; Golomb, M. C.; Mirkin, C. A.; Kaplan, D. L. *Proc. Natl. Acad. Sci. U.S.A.* **2001**, *98*, 13660−13664.
(43) Agarwal, G.; Sowards, L. A.; Naik, R. R.; Stone, M. O. *J. Am. Chem. Soc.* **2003**, *125*, 580−583.
(44) Demers, L. M.; Ginger, D. S.; Park, S. J.; Li, Z.; Chung, S. W.; Mirkin, C. A. *Science* **2002**, *296*, 1836−1838.
(45) Zhang, H.; Li, Z.; Mirkin, C. A. *Adv. Mater.* **2002**, *14*, 1472−1474.
(46) Smith, J. C.; Lee, K. B.; Wang, Q.; Finn, M. G.; Johnson, J. E.; Mrksich, M.; Mirkin, C. A. *Nano Lett.* **2003**, *3*, 883−886.
(47) Cheung, C. L.; Camerero, J. A.; Woods, B. W.; Lin, T.; Johnson, J. E.; DeYoreo, J. J. *J. Am. Chem. Soc.* **2003**, *125*, 6848−6849.
(48) Takeda, S.; Nakamura, C.; Miyamoto, C.; Nakamura, N.; Kageshima, M.; Tokumoto, H.; Miyake, J. *Nano Lett.* **2003**, *3*, 1471−1474.
(49) Nam, J. M.; Han, S. W.; Lee, K. B.; Liu, X.; Ratner, M. A.; Mirkin, C. A. *Angew. Chem., Int. Ed.* **2004**, *43*, 1246−1249.
(50) Tassew, N.; Thompson, M. *Anal. Chem.* **2002**, *74*, 5313−5320.
(51) Fawell, S.; Seery, J.; Daikh, Y.; Moore, C.; Chen, L. L.; Pepinsky, B.; Barsoum, J. *Proc. Natl. Acad. Sci. U.S.A.* **1994**, *91*, 664−668.
(52) Long, K. S.; Crothers, D. M. *Biochemistry* **1999**, *38*, 10059−10069.
(53) Long, K. S.; Crothers, D. M. *Biochemistry* **1995**, *34*, 8885−8895.
(54) Niesner, U.; Halin, C.; Lozzi, L.; Gunthert, M.; Neri, P.; Wunderli-Allenspach, H.; Zardi, L.; Neri, D. *Bioconjugate Chem.* **2002**, *13*, 729−736.
(55) Lewin, M.; Carlesso, N.; Tung, C. H.; Tang, X. W.; Cory, D.; Scadden, D. T.; Weissleder, R. *Nature Biotech.* **2000**, *18*, 410−414.
(56) Kurth, D. G.; Bein, T. *Langmuir* **1993**, *9*, 2965−2973.
(57) Lateef, S. S.; Boateng, S.; Hartman, T. J.; Crot, C. A.; Russell, B.; Hanley, L. *Polym. Mater. Sci. Eng.* **2001**, *85*, 403−404.
(58) Lateef, S. S.; Boateng, S.; Hartman, T. J.; Crot, C. A.; Russell, B.; Hanley, L. *Biomaterials* **2002**, *23*, 3159−3168.
(59) Rezania, A.; Johnson, R.; Lefkow, A. R.; Healy, K. E. *Langmuir* **1999**, *15*, 6931−6939.
(60) Xiao, S.-J.; Textor, M.; Spencer, N. D. *Langmuir* **1998**, *14*, 5507−5516.
(61) Hong, H. G.; Jiang, M.; Sliger, S. G.; Bohn, P. W. *Langmuir* **1994**, *10*, 153−158.
(62) Oh, S. J.; Cho, S. J.; Kim, C. O.; Park, J. W. *Langmuir* **2002**, *18*, 1764−1769.
(63) Maubach, G.; Fritzsche, W. *Nano Lett.* **2004**, *4*, 607−611.
(64) Jang, J.; Hong, S.; Schatz, G. C.; Ratner, M. A. *J. Chem. Phys.* **2001**, *115*, 2721−2729.
(65) Banerjee, D.; Amro, N. A.; Flagala, J. *Proc. SPIE (Microfluidics, BioMEMS, and Medical Microsystems II)* **2004**, *5345*, 230−237.
(66) Castner, D. G.; Ratner, B. D. *Surf. Sci.* **2002**, *500*, 28−60.
(67) Weeks, K. M.; Crothers, D. M. *Biochemistry* **1992**, *31*, 10281−10287.